

Structure and twinning of tetragonal $\text{Ca}_3\text{Mn}_2\text{Ge}_3\text{O}_{12}$ garnet

STEFAN HEINEMANN^{1,2,*} AND RONALD MILETICH^{1,†}

¹Bayerisches Geoinstitut, Universität Bayreuth, D-95440 Bayreuth, Germany

²Laboratoire de Structure et Propriétés de l'Etat Solide, Université des Sciences et Technologies de Lille, Cité Scientifique, 59655 Villeneuve d'Ascq Cedex, France

ABSTRACT

Single crystals of tetragonal $\text{Ca}_3\text{Mn}_2\text{Ge}_3\text{O}_{12}$ garnet (space group symmetry $I4_1/a$, $a = 12.3098(7)$ Å, $c = 12.3277(9)$ Å) were characterized by X-ray diffraction and transmission electron microscopy. Their structure is topologically isosymmetric to tetragonal high-pressure garnets such as majorite, displaying the same two distinct types of macroscopic twin mechanisms. Twinning occurs as pseudo-merohedral ferroelastic twin lamellae with preferred orientation of the twin-domain boundaries parallel to $\{101\}_{\text{tet}}$, whereas merohedral ferroblastic twin domains occur without any orientational preference. The crystal structure was determined from single-crystal X-ray diffraction data of a crystal fragment completely free of pseudo-merohedral twin domains. It shows two different Jahn-Teller distorted MnO_6 octahedra, with a different orientation of the axis of polyhedral elongation. The ordering scheme of these Jahn-Teller distorted octahedra follows in an alternating pattern the densest rod packing, and the cooperative effect of the electronically induced octahedral distortion was found to be responsible for the cubic-to-tetragonal symmetry breaking in $\text{Ca}_3\text{Mn}_2\text{Ge}_3\text{O}_{12}$ garnet. The extent of polyhedral distortion indicates a partially dynamic character of the Jahn-Teller effect. The distortion of the tetrahedral T2 sites controls the cooperative effect of the lattice strain induced by the Jahn-Teller distortion of the Mn^{3+} octahedra and thus is responsible for the overall lower symmetry.

INTRODUCTION

Garnets are known to be generally cubic according to $Ia\bar{3}d$ space-group symmetry. Nevertheless, the occurrence of birefringent (Hofmeister et al. 1998) and of non-cubic garnets has been reported (Deer et al. 1982), e.g., tetragonal symmetry has been found for the garnet-type structure of the high-pressure silicates $\text{Mg}_4\text{Si}_4\text{O}_{12}$ (= majorite; Angel et al. 1989) and $\text{Mn}_4\text{Si}_4\text{O}_{12}$ (Fujino et al. 1986), and analogous germanate compounds (Prewitt and Sleight 1969; Ross et al. 1986). Griffen and Hatch (1992) developed a model invoking phase transitions from cubic to a lower symmetry to be responsible for the occurrence of non-cubic garnets. As shown by Heinemann et al. (1997) for tetragonal majorite-pyropo garnet solid solutions, a cubic-to-tetragonal phase transition occurs at both high pressures and temperatures, as deduced from symmetry analysis and the investigation of the twin domain microstructure. An analogous cubic-to-tetragonal transition has been reported for $\text{Ca}_3\text{Mn}_2\text{Ge}_3\text{O}_{12}$ (CMG) (Kazei et al. 1977), which occurs, in contrast to the high-pressure silicate garnets, at ambient pressure thus serving as an analogue for majorite with respect to the macroscopic properties of the transition. The microscopic mechanisms and driving forces of the transition certainly are

different in nature, because order-disorder of Mg and Si on the octahedral site accounts for the phase transition in majorite (Angel et al. 1989), which is not a viable mechanism for CMG.

Symmetry breaking in CMG has been attributed to the Jahn-Teller effect in the MnO_6 octahedron (Kazei et al. 1982) but, because of the lack of a reliable structure investigation, this has not yet been confirmed beyond doubt. CMG, in particular its optical properties, has attracted major interest in optical physics mostly because of the material's photorefractive effect below ca. 200 K and the possible technical application for holographic recording (Sugg et al. 1995; 1996). Powder neutron and X-ray diffraction studies (Plumier 1971; Breuer and Eysel 1983) showed CMG to be of apparent cubic $Ia\bar{3}d$ symmetry. In contrast, optical investigations on (twinned) single crystals revealed birefringence to occur for temperatures below 516 K (Gnatchenko et al. 1986). Kazei et al. (1977, 1982) demonstrated by single-crystal X-ray diffraction that the symmetry changes from cubic to tetragonal at 525K, but investigations did not include a full crystal-structure determination. The symmetry at room temperature was assumed to be $4/m$ (Eremenko et al. 1986; Kharchenko and Bedarev 1993), and space-group symmetry was reported to be $I4_1/a$ (Gnatchenko et al. 1986) or $I4_1/acd$ (Toledano and Toledano 1987) respectively. Investigations by polarization microscopy (Gnatchenko et al. 1986) and synchrotron X-ray topography (Graeff et al. 1991) revealed that the domain walls of the twins are parallel to the former cubic planes $\{110\}_{\text{cub}}$ and tetragonal planes $\{110\}_{\text{tet}}$, $\{011\}_{\text{tet}}$. Merohedral domains such as observed for tetragonal majorite

*Present address: GeoForschungsZentrum Potsdam, D-14473 Potsdam, Germany. E-mail: stefan.heinemann@gfz-potsdam.de

†Present address: Laboratory for Crystallography, ETHZ, CH-8092 Zürich, Switzerland.

garnets of symmetry $I4_1/a$ (Heinemann et al. 1997) have not been reported in this X-ray topography study. Their absence was the basis to argue for $I4_1/acd$ space group symmetry, which is in contrast to the previous investigations.

Although the optical properties of CMG are quite well understood, the true symmetry is therefore still a matter of discussion and the crystal structure has not yet been determined experimentally. Here we report the results of X-ray diffraction and transmission-electron microscopy studies on twinned and untwinned single crystals, which allow the complete crystal-structure determination of CMG for the first time. These studies are complemented by the characterization of the microstructure with respect to the occurrence of providing important information to determine the true symmetry.

CRYSTAL GROWTH AND SAMPLE PREPARATION

Crystals were synthesized from a lead-bearing flux in a platinum crucible, using a starting mixture containing 44 mol% PbO (99.9%, Aldrich), 15 mol% CaCO_3 (99.9%, Heraeus), 6 mol% Mn_2O_3 (99.9%, ChemPur) and 35 mol% 99.9% GeO_2 , (Ventron/AlfaProducts) (Desvignes and LeGall 1978). The melt was cooled from 1300 to 800 °C in a vertical temperature gradient at a constant cooling rate of 3 °C/h. $\text{Ca}_3\text{Mn}_2\text{Ge}_3\text{O}_{12}$ garnet single crystals between 2 mm and 20 mm in size were obtained at the top of the crucible. The bottom of the crucible contained a fine grained intergrowth of garnet, $\text{Pb}_{11}\text{Ge}_3\text{O}_{17}$ and GeO_2 . Synthesis products have been analyzed using a CAMECA SX50 electron microprobe in wavelength dispersive mode with a beam diameter 10–20 μm . Samples were coated with carbon and analyzed with 20 kV acceleration voltage and a 20 nA current. Andradite (Ca), pyrophanite (Mn), germanium (Ge), and vanadinite (Pb) served as standards for the elements given in parentheses. The average composition of the garnet single crystals reflects a $^{181}(\text{Ca}_{2.963(25)}\text{Pb}_{0.004(3)})^{161}\text{Mn}_{2.049(23)}^{141}\text{Ge}_{2.981(34)}\text{O}_{12.003(12)}$ composition, which is very close to the stoichiometric end member garnet composition. It is remarkable that all analyses of the individual crystals from this batch revealed homogeneous compositions and only insignificantly small amounts of lead.

A centimeter-sized crystal was oriented by oscillation-film photographs within $\pm 0.3^\circ$ orientational error. After embedding in epoxide resin, an oriented $\{100\}_{\text{cub}}$ platelet, 32 μm in thickness and 4 mm \times 4 mm in lateral size, was cut from the crystal and polished on both sides. Optical microscopy investigations under crossed polarizers revealed an approximately 2–3 mm² large crystal domain which was absolutely free of any twin lamellae. A 140 μm \times 60 μm fragment, broken from this region, was used for the single-crystal X-ray diffraction study. The remaining mainly twinned parts were used for the transmission electron microscopy (TEM) investigations. They were mounted on a 3 mm diameter Pt grid using high temperature epoxy glue (EPO-TEK 377) and mechanically thinned to approximately 10 μm using a Gatan Dimple Grinder. Final ion thinning was performed using a Gatan Duomill 600 with Ar ions (5 kV, 15° to the sample surface) until holes with electron-transparent rims were formed. Samples were coated with 5 to 10 nm of amorphous carbon to prevent charging in the electron microscope. The mounted sample was heated above 350 °C for 2 min to relax any mechanical strains from the preparation procedure.

TRANSMISSION ELECTRON MICROSCOPY: SYMMETRY AND TWINNING

TEM investigations were performed using a 200 kV Philips CM20FEG and a 300 kV Philips CM30 microscope equipped with a LaB_6 cathode and double-tilt sample holders. The deviation from cubic symmetry is reflected both by systematic extinctions in the selected area electron diffraction (SAED) patterns and in the microtextures, particularly by the presence of twin domains. The violation of the $h + l = 4n$ extinction rule for (hhl) reflections and the resulting electron diffraction extinction symbol $I_{-}a_{-}$ indicate that the d glide plane (accord-

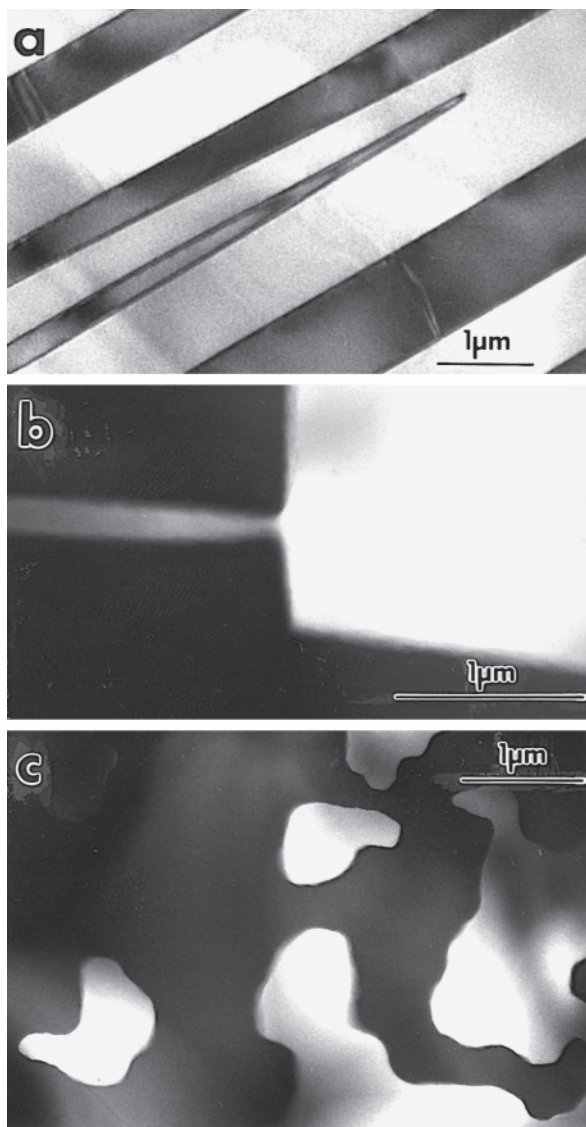


FIGURE 1. Twin Domains in tetragonal $\text{Ca}_3\text{Mn}_2\text{Ge}_3\text{O}_{12}$ garnet. (a) Parallel ferroelastic domains and needles parallel $\{101\}_{\text{tet}}$. (b) Perpendicular ferroelastic domain boundaries with single 90° junction and pair of 90° junction. (c) Ferroelastic domains with curved domain walls without preferred orientation.

ing to the cubic $Ia\bar{3}d$ symmetry) is absent due to the symmetry breaking.

In total two merohedral (Fig. 1c) and three pseudo-merohedral twin domains (Figs. 1a and 1b) of different orientation have been observed in CMG, similar to those reported for majorite and tetragonal majorite-pyrope solid solutions (Angel et al. 1989; Heinemann et al. 1997). Significant contrast for imaging the pseudo-merohedral twin domains can only be achieved for reflections (hkl) with $h \neq l$, $k \neq l$. For merohedral twins contrast is observed only for reflections (hkl) with $h \neq k$ where there is a significant difference between the hkl and khl structure factor; for the symmetry-equivalent reflections (hhl), (hOl) \leftrightarrow (Okh) and ($h00$) \leftrightarrow ($0k0$), no merohedral contrasts are observed. Merohedral twins do not show optical contrast with crossed polarizers. Mirror planes for the pseudo-merohedral twins are the cubic $(101)_{\text{cub}}$, $(10\bar{1})_{\text{cub}}$, $(011)_{\text{cub}}$, and $(01\bar{1})_{\text{cub}}$ planes = $\{101\}_{\text{tet}}$, whereas for merohedral twinning $(110)_{\text{cub}}$ and $(1\bar{1}0)_{\text{cub}}$ planes = $\{110\}_{\text{tet}}$ are the twin-generating symmetry operators. Again, this is consistent with space group $I4_1/a$ because the cubic mirror planes relating the twins are not mirror planes in this tetragonal space group.

Griffen and Hatch (1992) analyzed supergroup-subgroup relationships and showed ten possible ways for cell-preserving phase transitions of garnets which are driven by a single order parameter. Two possible phase transitions result in a tetragonal space group symmetry: $I4_1/acd$ or $I4_1/a$. Theoretically, in $I4_1/acd$ three domains of different orientation and in $I4_1/a$ six domains occur. The six domains in tetragonal CMG are the result of a combination of the three pseudo-merohedral twin domains and the two merohedral domains, which is consistent with space group $I4_1/a$. The terms which refer to the origin of the twins at the phase transition are ferroelastic domains for pseudo-merohedral twins and ferrobielastic domains for merohedral twins (Salje 1990).

The exchange of the unequal a and c axes by ferroelastic domain boundaries causes strain in the crystal and the preferred orientation of the ferroelastic domain walls (Sapriel 1975) parallel to the four tetragonal planes $\{101\}_{\text{tet}}$ = $(101)_{\text{tet}}$, $(10\bar{1})_{\text{tet}}$, $(011)_{\text{tet}}$, $(01\bar{1})_{\text{tet}}$, but not parallel to $(110)_{\text{tet}}$, $(1\bar{1}0)_{\text{tet}}$. The orientational arrangement of all three possible ferroelastic domains expressed in pseudo-cubic symmetry is given by the six cubic mirror planes $\{101\}_{\text{cub}}$ = $(110)_{\text{cub}}$, $(1\bar{1}0)_{\text{cub}}$, $(101)_{\text{cub}}$, $(10\bar{1})_{\text{cub}}$, $(011)_{\text{cub}}$, $(01\bar{1})_{\text{cub}}$. Due to these preferred orientations domains occur as parallel lamellae or needles (Fig. 1a). Non-parallel domain boundaries appear as single or paired 90° junctions (Fig. 1b) and the paired 90° junctions merge into needles (Palmer et al. 1988). Ferrobielastic domains, in contrast to the ferroelastic domains, result in the superposition of equal lattice parameters and do not produce ferroelastic lattice strain. The ferrobielastic twin boundaries are therefore not constrained to planes of minimum strain and tend to be curved and irregular (Fig. 1c).

SINGLE-CRYSTAL X-RAY DIFFRACTION

X-ray diffraction intensities were collected (at room temperature, 21 °C, in air) on a Nonius CAD4 four-circle diffractometer with graphite-monochromatized MoK α radiation ($\lambda = 0.7103$ Å) with a tube power of 50 kV and 50 mA. X-ray intensities were collected to $(\sin\theta)/\lambda \leq 0.807$ Å⁻¹ within

one quarter of the reciprocal space ($0 \leq h, k \leq 19$, $-19 \leq l \leq 19$) by ω -2 θ scans (scan width: $0.66 + 0.35^\circ \tan \theta$; scan time: 12 to 240 s). The (4 0 2), (0 4 2), ($\bar{2}4\bar{6}$) standard reflections served as intensity and orientation control every 2 h and showed no systematic variation with time. Integrated intensities were obtained from the scan data using a modified Lehmann-Larsen algorithm (Grant and Gabe 1978). Intensities of all measured reflections were corrected for Lp and crystal absorption effects. The numerical absorption correction by Gaussian integration according to the optically determined crystal shape was carried out with a modified version of ABSORB (Burnham 1966). Data reduction indicated that reflections with h , k odd in $hk0$ and $l \neq 4n$ were absent, and the space group was therefore uniquely determined to be $I4_1/a$. Averaging according to Laue symmetry $4/mmm$ revealed R_{int} to be 16.6%. Moreover, significant intensities were observed for reflections both with k , $l \neq 2n$ in $0kl$ and $2h + l \neq 4n$ for hhl which ruled out $I4_1/acd$ symmetry. All symmetry-allowed reflections were averaged using the criteria of Blessing (1987). Structure refinements were carried out with RFINE90, a development version of RFINE4 (Finger and Prince 1975). A weight of $w = [\sigma^2(F_o) + (0.003 F_o)^2]^{-2}$ was assigned to each observed reflection, where $\sigma(F_o)$ was derived from counting and averaging statistics. The positional parameters of the cubic garnet structure (Novak and Gibbs 1971) transformed to $I4_1/a$ symmetry were used as starting model. In conformity with the $Ia\bar{3}d$ symmetry elements of cubic garnets, the origin was shifted by 1/2,0,0 relative to the origin of $I4_1/a$ setting 2 at the Wyckoff position 8c. Complex scattering factors for neutral atoms as well as the linear mass-absorption coefficients were taken from the *International Tables of Crystallography* (Maslen et al. 1992; Creagh and McAuley 1992). Refinements included a correction for secondary isotropic extinction (Lorentzian type-I; Becker and Coppens 1974). A refinement with mixed occupancies according to a possible (but very minor) substitution of Pb on the dodecahedral and octahedral sites revealed that Pb does not substitute significantly either for Ca and Mn on these sites. Results of the least-squares refinements are given in Table 1, the refined structural parameters are summarized in Table 2. Single-crystal unit-cell parameters were determined from the setting angles of 36 reflections (cubic classes {400}, {800}, {024}, {246}, {248}; $13.2^\circ \leq 2\theta \leq 30.6^\circ$) determined on a Huber four-circle diffractometer operated with non-monochromatized Mo radiation. Precise setting angles were by fitting Gaussian profiles to the final scans in χ and ω (Angel et al. 1997). To eliminate crystal-offset errors and diffractometer aberrations, the technique of diffracted beam centering (King and Finger 1979) was employed. Unit-cell parameters (Table 1) were obtained from a vector-least squares fit (Ralph and Finger 1982) to these corrected reflection positions.

CRYSTAL STRUCTURE DESCRIPTION

The structure refinement from X-ray single-crystal diffraction data confirms the garnet-aristotype crystal structure. High-precision lattice parameters clearly show the CMG garnet to be of tetragonal symmetry with the c axis being 0.1% larger than a [$c/a = 1.001238(6)$]. According to the $^{18}\text{X}_3^{16}\text{Y}_2^{14}\text{Z}_3\text{O}_{12}$ formula for garnets (Novak and Gibbs 1971), $I4_1/a$ space-group

TABLE 1. Crystal data, and details of the data reduction and least squares refinement for Ca₃Mn₂Ge₃O₁₂ garnet

<i>a</i> (Å)	12.3098(7)	Space group	<i>I</i> ₄ / <i>a</i> , 2nd setting
<i>c</i> (Å)	12.3277(9)	<i>Z</i>	8
<i>V</i> (Å ³)	1868.031(23)	ρ_{calc} (g/cm ³)	4.55
Dimensions (μm^3)	140 × 60 × 32	$\lambda_{\text{MoK}\alpha}$ (Å)	0.7103
$2\theta_{\text{max}}$ (°)	70	$\mu_{\text{MoK}\alpha}$ (cm ⁻¹)	136.33
N_{ref} (+ <i>h</i> , + <i>k</i> , ± <i>l</i>)	4393	R_{int}	0.026
N_{unique} ($F > 0.5\sigma_F$)	2045	R	0.031
N_{obs} ($F > 4\sigma_F$)	941	RW	0.034
N_{var}	95	σ	$6.3(1.2) \times 10^{-2}$
<i>t</i> (%)	49.8–66.1	G_{int}	1.08

symmetry requires an increase of the number of symmetry independent dodecahedral (⁸X = D), octahedral (⁶Y = Oc), and tetrahedral (⁴Z = T) sites. According to symmetry breaking, individual sites have different site symmetries for the two DO₈ ($\bar{1}, 2..$), three TO₄ ($2 \times \bar{4}, 1$) and two OcO₆ (both $\bar{1}$) polyhedra, instead of one type each of dodecahedral, tetrahedral, and octahedral sites with the respective point symmetries $2, \bar{4},$ and $\bar{3}$ in cubic garnet. In the following discussion the site notation refers to D, Oc, and T for the type polyhedron in the aristotype structure, numbers (1, 2, ...) and letters (a, b) reflecting site creation through the individual $Ia\bar{3}d \rightarrow I4_1/acd$ and $I4_1/acd \rightarrow I4_1/a$ steps of symmetry breaking. The a and b sites merge for $I4_1/acd$ symmetry only and 1, 2, ... sites merge for $Ia\bar{3}d$ symmetry only.

Although of different symmetry, the topological connectivity remains unchanged relative to that of regular cubic garnets (Fig. 2), thus accounting for a true displacive nature for the tetragonal-to-cubic transition at high temperatures. This is in contrast to the (on a macroscopic scale) apparently equivalent transition in majorite which is known to result from an order-disorder mechanism (Angel et al. 1989; Heinemann et al. 1997). The lack of rigid-unit modes which has been recently evaluated for the garnet structure-type (Hammonds et al. 1998), means that symmetry-breaking transitions cannot occur without changes in the polyhedral geometries. As all types of D, Oc, and T sites are each occupied by one atomic sort only, namely Ca on D, Mn on Oc, and Ge on the T sites, the elec-

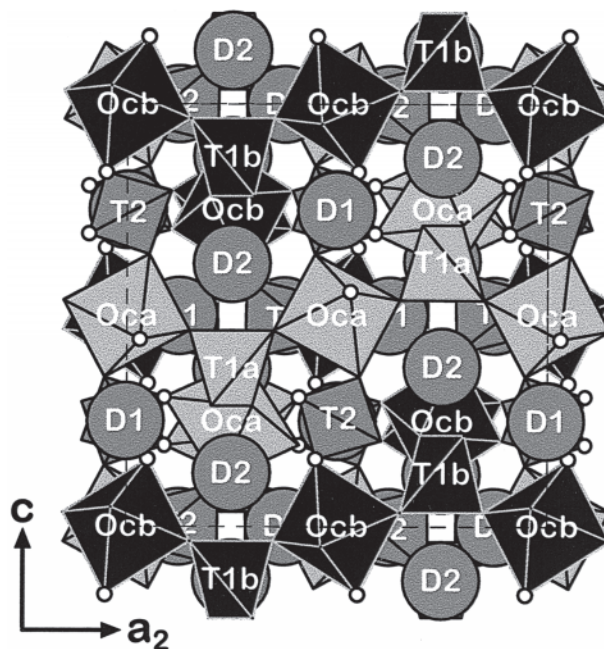


FIGURE 2. Tetragonal structure of Ca₃Mn₂Ge₃O₁₂ garnet. The sub-frameworks a (light gray) and b (black) of corner-sharing GeO₄ tetrahedra and MnO₆ octahedra (Oca, T1a and Ocb, T1b) are corner-connected by the bridging tetrahedron T2 (dark gray). The long axis of the Jahn-Teller distorted MnO₆ octahedra Oca and Ocb is marked with the adjoining oxygen atoms O2a and O3b. In the voids between the corner sharing sub-frameworks is Ca in dodecahedral coordination (D1 and D2, dark gray).

tronically induced polyhedral distortion, that is the Jahn-Teller effect of the Mn³⁺ cations, must be the driving force for the overall symmetry change in CMG.

Jahn-Teller effect and polyhedral geometries

The 3d⁴ electronic configuration of transition-metal cations in octahedral fields leads to a singular occupation of the two-fold degenerate e_g level in a regular coordination geometry.

TABLE 2. Positional and thermal displacement parameters from the refinement of Ca₃Mn₂Ge₃O₁₂ garnet

Site	Site Sym.	Atom	<i>x</i>	<i>y</i>	<i>z</i>	β_{11}	β_{22}	β_{33}	β_{12}	β_{13}	β_{23}	β_{eq}
D1	1	Ca	0.12510(12)	-0.00229(11)	0.25040(10)	132(7)	177(8)	149(7)	4(6)	-5(5)	17(5)	0.927
D2	2	Ca	0	1/4	0.62281(13)	195(10)	170(10)	107(8)	-27(8)	0	0	0.955
Oca	$\bar{1}$	Mn	0	0	1/2	131(8)	121(8)	112(8)	12(7)	-4(6)	0(5)	0.736
Ocb	$\bar{1}$	Mn	0	0	0	115(8)	126(8)	120(6)	12(6)	-10(6)	1(6)	0.730
T1a	$\bar{4}$	Ge	0	1/4	3/8	156(5)	107(7)	107(7)	0	0	0	0.846
T1b	$\bar{4}$	Ge	0	1/4	7/8	175(5)	= β_{11}	96(7)	0	0	0	0.901
T2	1	Ge	0.12518(6)	0.00317(6)	0.74330(6)	120(4)	145(4)	135(4)	-5(3)	-2(3)	-1(3)	0.808
O1a	1	O	0.45180(40)	0.64970(40)	0.96420(40)	198(28)	176(24)	144(25)	-52(21)	-10(22)	39(22)	1.048
O1b	1	O	0.05220(40)	0.65290(40)	0.03340(40)	200(27)	195(28)	144(25)	3(21)	-35(23)	-37(22)	1.089
O2a	1	O	0.66010(40)	0.03110(40)	0.05690(40)	116(25)	171(27)	205(27)	-8(20)	22(22)	-23(22)	0.994
O2b	1	O	0.85580(40)	0.03720(40)	0.95380(40)	147(26)	157(26)	181(25)	50(20)	-4(22)	7(22)	0.982
O3a	1	O	0.03190(40)	0.05270(40)	0.64520(40)	140(24)	190(27)	131(23)	-23(20)	-18(20)	-23(20)	0.931
O3b	1	O	0.46480(40)	0.04990(40)	0.33990(40)	194(28)	221(28)	159(26)	-9(23)	4(23)	-38(23)	1.160

Notes: Site labels were chosen as the garnet site notation (D = dodecahedron, Oc = octahedron, T = tetrahedron, O = oxygen). Origin of atomic coordinates shifted by 1/2, 0, 0 relative to standard site origin of setting 2 (at Wyckoff position 8c), to achieve conformity with the atomic positions of cubic garnets and previous descriptions of tetragonal garnets. Anisotropic displacement parameters β_j are given in the form $\exp[-(\frac{1}{2}\beta_{11} + \frac{1}{2}\beta_{22} + \frac{1}{2}\beta_{33} + 2h\beta_{12} + 2h\beta_{13} + 2k\beta_{23})]$. β_j values are multiplied by 10⁵.

The direct electrostatic interaction between the coordinating ligands and the electrons within the two orbital $d_{x^2-y^2}$ and d_{z^2} thus produces a spontaneous distortion of the co-ordination geometry which results in a removal of the degeneracy and the stabilization of the single e_g electron at a lower energy level (Jahn and Teller 1937; Englman 1972). Following the geometry and orientation of d-electron orbitals, the effect of polyhedral distortion that results in a more stable electronic configuration is either a uniaxial elongation or a compression along one of the axes of the octahedron. This reduces the theoretical $m\bar{3}m$ point symmetry of a regular octahedral geometry to $4/m\bar{3}m$ symmetry or subgroups of it. Accordingly, the $\bar{3}$ symmetry of the octahedral position in cubic garnet is certainly not compatible with the symmetry requirements to fulfill the Jahn-Teller theorem.

Because the favored polyhedral distortion for Mn^{3+} is incompatible with the garnet site symmetry, the incorporation of Mn^{3+} into the Y-site in the cubic garnet structure was repeatedly disputed (Strens 1965; Rickwood 1968). Mn^{3+} bearing cubic garnets, $\text{Ca}_3\text{Mn}_2\text{Si}_3\text{O}_{12}$ and $\text{Cd}_3\text{Mn}_2\text{Si}_3\text{O}_{12}$, were first synthesized by Nishizawa and Koizumi (1975), later Fursenko (1983) synthesized $\text{Mn}_3\text{Mn}_2\text{Si}_3\text{O}_{12}$ (=blythite) which was proved by single-crystal diffraction to be of cubic symmetry at various temperatures and pressures (Arlt et al. 1998). The structure refinements revealed a disordered Jahn-Teller distortion either of dynamic or static nature as evidenced by unusually high displacement parameters, confirming previous conclusions made by Arni et al. (1985).

The structure refinement of CMG shows uniaxial distortions of both octahedral sites (Oca and Ocb: Figs. 3a and 3b, Table 3). The average Mn-O bond distances [Oca: 2.019(4) Å, Ocb: 2.021(4) Å] are very similar to that of the Fe^{3+} -O bond distance [2.017(3) Å] in $\text{Ca}_3\text{Fe}_2\text{Ge}_3\text{O}_{12}$ (CFG) garnet, which in contrast represents an undistorted garnet structure of ideal cubic symmetry (Prandl 1972) and equal metric [radius of $^{VI}\text{Mn}^{3+}(\text{HS})$ = radius of $^{VI}\text{Fe}^{3+}(\text{HS})$; Shannon 1976]. The relative distortions of the bond length on both Oc sites in tetragonal CMG relative to the Oc site in cubic CFG are combination of axial elongation (O2a-Oc-O2a) and equatorial compressions (O1a-Oca-O1a, O3a-Oca-O3a) for Oca with an axial compression (O2b-Ocb-O2b) and equatorial elongations (O1b-Ocb-O1b, O3b-Ocb-O3b) for Ocb. Whereas the absolute distortion effects on both Oc sites in CMG correspond to the usual octahedral elongations resulting in a 4 + 2 configuration (Table 3) of two longest (Oca-O2a, Ocb-O3b) and four short Mn-O bonds (Oca-O1a, Oca-O3a; Ocb-O1b, O2b-O2b) (Shannon et al. 1975).

For fully ordered Mn^{3+} -bearing oxide phases such as e.g., hausmannite (Mn_3O_4 ; Jarosch 1987) or braunite ($\text{Mn}_7\text{SiO}_{12}$; Miletich et al. 1998) the uniaxially elongated bond is ~15–20% longer relative to the four equatorial Mn-O bonds (see also Shannon et al. 1975; Hoffmann et al. 1997, and references therein). The distortion of the two octahedra in CMG is considerably smaller with the longest axial Mn-O bond lengths being elongated by ~10%, respectively. Both the extent of uniaxial elongation relative to that observed in other MnO_6 octahedra and the apparently larger displacement parameters of the oxygen atoms in comparison to other cubic garnet struc-

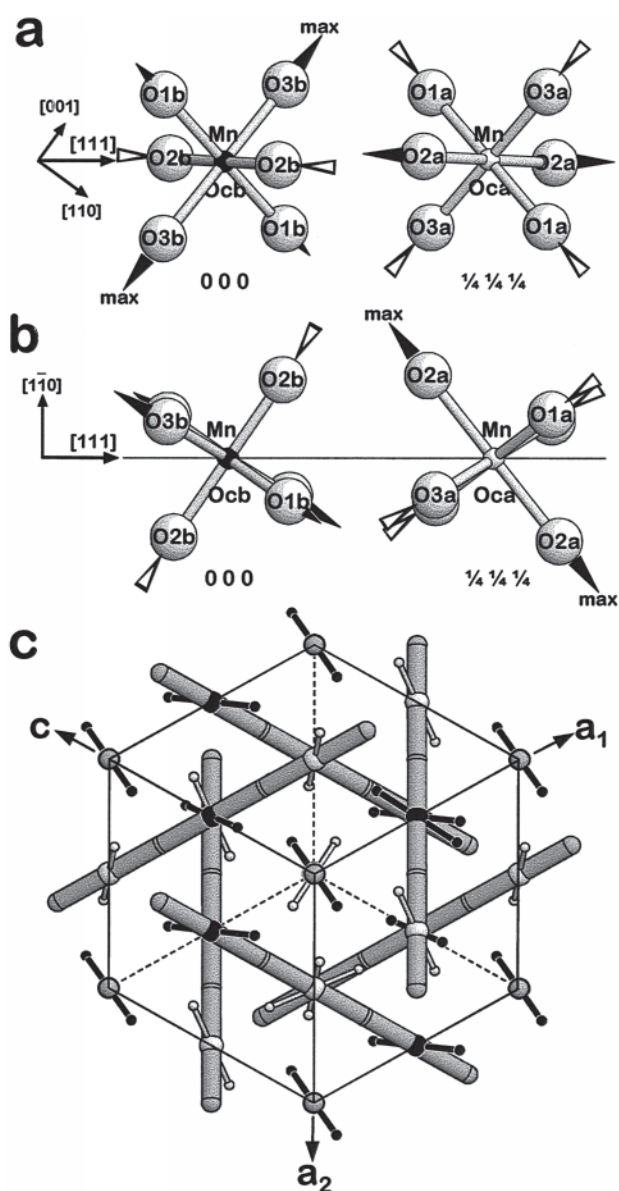


FIGURE 3. Jahn-Teller distorted MnO_6 -octahedra Oca and Ocb along $\{111\}$. View of $[111]$ perpendicular to $[1\bar{1}0]$ (a) and $[11\bar{2}]$ (b). All $\{111\}$ directions in the unit cell viewed along $[111]$ (c). (a and b) Alternating Jahn-Teller distorted MnO_6 octahedra. The longest axis of the octahedra Oca and Ocb are O2a-Oca-O2a and O3b-Ocb-O3b (max). The arrows indicate the shifts relative to the undistorted octahedron in cubic $\text{Ca}_3\text{Fe}_2\text{Ge}_3\text{O}_{12}$ garnet. (c) Ordering scheme of alternating Jahn-Teller distorted MnO_6 octahedra Oca (light gray) and Ocb (black) at non-intersecting rods along $\{111\}$. Unit cell viewed along its diagonal $[111]$. The directions of ordering are indicated by thick gray rods. The longest octahedral axis are marked by single white (O2a-Oca-O2a) or black (O3b-Ocb-O3b) axis.

tures (e.g., Armbruster and Geiger 1993) suggest the partial disorder character, which accounts in cubic Mn³⁺ bearing garnets (Nishizawa and Koizumi 1975; Fursenko 1983; Arni et al. 1985; Arlt et al. 1998) for the suppression of the polyhedral distortion in X-ray diffraction.

The cooperative effect of distortion

The ordering scheme of alternating different distorted MnO₆ octahedra Oca and Ocb along the former cubic threefold axes follows the structure model of the densest packing of non-crossing rods in cubic garnets (Andersson and O'Keefe 1977). Oca and Ocb alternate along $n \cdot [111]$, $n \cdot [1\bar{1}\bar{1}] + [1/2\ 0\ 1/2]$, $n \cdot [1\bar{1}\bar{1}] + [0\ 1/2\ 1/2]$ and $n \cdot [\bar{1}\bar{1}\bar{1}] + [1/2\ 1/2\ 0]$ and the other equivalent directions, with $n = \{0, 1/2\}$ for Ocb and $n = \{1/4, 3/4\}$ for Oca (Fig. 3c). This ordering scheme is equal to the antiferromagnetic spin order in CMG below 13.5 K (Plumier and Estève 1979) so that the Jahn-Teller ordering pattern acts as a precursor for the magnetic structure. The ordering principle is the same for the cation ordering of tetragonal high-pressure silicate and germanate garnets (Angel 1989; Fujino et al. 1986; Prewitt and Sleight 1969; Ross et al. 1986).

The Oc-octahedron in the garnet structure does not share any common edges or corners with other OcO₆ octahedra. Polyhedral interconnectivity is achieved by linkages through the dodecahedral and tetrahedral sites. Although the Oc-site can thus be said to be isolated with respect to exclude a direct cooperative Jahn-Teller effect, the tetragonal symmetry indicates

that the local lattice strains induced by the Jahn-Teller distortion interact in a coordinated form which leads to the symmetry breaking of the overall structure. This kind of cooperative effect, which usually is known for direct interactions between neighboring polyhedra in polymerized units, such as in edge-sharing chains (Hoffmann et al. 1997), can be expected to be mediated by the DO₈ and TO₄ polyhedra in the case of the garnet structure.

The key role for understanding the absence of an overall symmetry change of the structure in cubic Mn³⁺ bearing silicate garnets (Fursenko 1983; Arni et al. 1985; Arlt et al. 1998), compared to the apparent cooperative distortion effect in CMG, can be attributed to the T sites. The symmetry $\bar{4}$ of site T1a and T1b within the sub-frameworks a and b is the highest symmetric site in the tetragonal CMG garnet structure and equals the T site symmetry in cubic garnet. Both T1a and T1b are coordinated by type O1 oxygen atoms (Fig. 4a,b). These O1a or O1b atoms are without exception equatorial oxygen atoms in the MnO₆ octahedra, i.e. they form short Mn-O bonds. The axial oxygen (O2a, O3b) atoms within both MnO₆ octahedra, which are those of the axis of polyhedral elongation and the equatorial atoms (O3a, O2b) which are those of the shortest octahedral axis (Table 3), belong to the T2 tetrahedron (Fig. 4c). This T2 tetrahedron with point symmetry 1, has the largest polyhedral distortion both in bond-distances (up to 9.6% as expressed by the ratio of long to short edges) and angular variations (up to 14.05° difference). It appears that the T2 site has to accommodate the local strain induced by the polyhedral elongation of the MnO₆ octahedra. Because the T2 site is acceptor of both axes of uniaxial elongation in the two individual Mn sites, namely the O2a-Oca-O2a and O3b-Ocb-O3b axes, it appears to be a cooperative effect of distortion linking the two types of octahedra along the *c*-axis. The Ge atom which is larger and therefore more flexible with respect to its stereo chemistry is better suited to accommodate strain-induced changes by distortion than the smaller and stiffer SiO₄ tetrahedra. The higher rigidity of the SiO₄ compared to the GeO₄ unit might be the most plausible explanation for why all known Mn³⁺ bearing silicate garnets with pure Jahn-Teller distortions preserve their cubic structure, whereas Ca₃Mn₃Ge₃O₁₂ adopts tetragonal symmetry.

Noncubic symmetries have also been reported for the OH-bearing natural garnet henritermiérite Ca₃(Mn_{0.75}Al_{0.25})₂Si₂(OH)₄O₈ (Aubry et al. 1969), for Mn₃(MnSi)Si₃O₁₂ (Fujino et al. 1986), for Mg₃(Mg_{0.34}Si_{0.34}Al_{0.18}Cr_{0.14})₂Si₃O₁₂ (Nakatsuka et al. 1999) and vanadate garnets [Ca₂Na]Mn₂V₃O₁₂ (palenzonaite: Basso 1987), [Ca₂Na]Cu₂V₃O₁₂ (Kazei et al. 1982). In all these cases the cooperative effect of the Jahn-Teller-active cations (Mn³⁺, Cr³⁺, Cu²⁺) is supported by ordering. In case of henritermiérite one third of the silicate atoms are substituted for an O₄H₄ hydrogrossular complex (Pabst 1936), whereas in the vanadate garnets one third of the divalent cations on the dodecahedral site has to be substituted by monovalent cations in order to balance stoichiometric charges. The possible effect of cation ordering in both cases support the symmetry-breaking which is also required from the Jahn-Teller theorem in order to accommodate the nonspherical cation shape by removing the incompatible site symmetry.

TABLE 3. Bond distances and angles of MnO₆-octahedra and GeO₄-tetrahedra

octahedron Oca			
Oca-O2a	2.127(4) Å	O2a-Oca-O1a	87.91(17) °
Oca-O1a	1.986(4) Å	O1a-Oca-O3a	87.44(18) °
Oca-O3a	1.944(4) Å	O3a-Oca-O2a	86.76(17) °
mean	2.019(4) Å	mean	87.37(17) °
octahedron Ocb			
Ocb-O3b	2.112(5) Å	O3b-Ocb-O2b	88.96(18) °
Ocb-O1b	2.031(5) Å	O1b-Ocb-O3b	89.13(17) °
Ocb-O2b	1.920(4) Å	O2b-Ocb-O1b	89.35(18) °
mean	2.021(5) Å	mean	89.15(18) °
tetrahedron T1a			
T1a-O1a	1.757(4) Å		
O1a-O1a	2.740(6) Å	O1a-T1a-O1a	102.49(20) °
O1a-O1a	2.931(6) Å	O1a-T1a-O1a	113.07(20) °
tetrahedron T1b			
T1b-O1b	1.765(5) Å		
O1b-O1b	2.714(6) Å	O1b-T1b-O1b	100.47(21) °
O1b-O1b	2.964(6) Å	O1b-T1b-O1b	114.15(21) °
tetrahedron T2			
T2-O2a	1.740(4) Å		
T2-O2b	1.785(4) Å		
T2-O3a	1.776(4) Å		
T2-O3b	1.753(5) Å		
mean	1.764(4) Å		
short edges			
O2a-O2b	2.725(6) Å	O2a-T2-O2b	101.27(20) °
O3a-O3b	2.713(6) Å	O3a-T2-O3b	100.49(21) °
mean	2.719(6) Å	mean	100.88(21) °
long edges			
O2a-O3a	2.955(6) Å	O2a-T2-O3a	114.37(20) °
O2a-O3b	2.938(6) Å	O2a-T2-O3b	114.54(21) °
O2b-O3a	2.975(6) Å	O2b-T2-O3a	113.37(20) °
O2b-O3b	2.957(6) Å	O2b-T2-O3b	113.42(21) °
mean	2.956(6) Å	mean	113.93(21) °

Notes: For tetrahedron T2, short and long tetrahedral edges are given also.

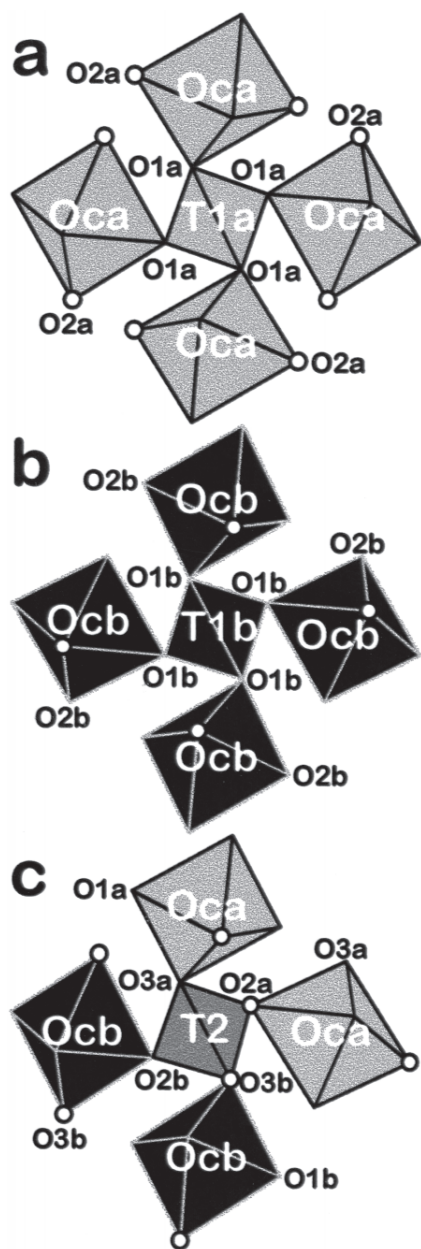


FIGURE 4. Tetrahedra and their octahedral surrounding. Tetrahedron T1a is symmetrically and only connected to the short octahedral axes O1a-Oca-O1a axes of Oca (a) and T1b only to the short axes O1b-Ocb-O1b of Ocb (b). Both tetrahedra viewed along c and tetrahedral $\bar{4}$. T2 is distorted by its connection to the longest octahedral axis (O2a-Oca-O2a, O3b-Ocb-O3b) and the short octahedral axes (O3a-Oca-O3a, O2b-Ocb-O2b) of both octahedra Oca and Ocb (c). T2 viewed along a and former tetrahedral $\bar{4}$.

ACKNOWLEDGMENTS

We thank Hubert Schulze for the careful preparation of the polished thin sections used for the TEM and X-ray investigations and Detlef Krause for the microprobe analysis. Furthermore, we would like to express our thanks to Friedrich Seifert, Thomas Armbruster, Lee Groat, and Anne M. Hofmeister for their critical reviews and constructive comments which greatly improved the manuscript. S.H. is grateful to the Fondation nationale Alfred Kastler de la l'Académie des Sciences for a postdoctoral fellowship, the kind care of CROUS de Lille and highly appreciates hospitality, discussions and assistance of Patrick Cordier.

REFERENCES CITED

- Andersson, S. and O'Keefe, M. (1977) Body-centered cubic cylinder packing and the garnet structure. *Nature*, 267, 605–606.
- Angel, R.J., Finger, L.W., Hazen, R.M., Kanzaki, M., Weidner, D.J., Liebermann, R.C., and Veblen, D.R. (1989) Structure and twinning of single-crystal MgSiO_3 garnet synthesized at 17 GPa and 1800 °C. *American Mineralogist*, 74, 509–512.
- Angel, R.J., Allan, D.R., Miletich, R., and Finger, L.W. (1997) The use of quartz as an internal pressure standard in high pressure crystallography. *Journal of Applied Crystallography*, 30, 461–466.
- Arlt, T., Armbruster, T., Miletich, R., Ulmer, P., and Peters, T. (1998) High pressure single-crystal synthesis, structure and compressibility of the garnet $\text{Mn}^{2+}_3\text{Mn}^{3+}_2[\text{SiO}_4]_3$. *Physics and Chemistry of Minerals*, 26, 100–106.
- Armbruster, T. and Geiger, C.A. (1993) Andradite crystal chemistry, dynamic X-site disorder and structural strain in silicate garnets. *European Journal of Mineralogy*, 5, 59–71.
- Arni, T.R., Langer, K., and Tillmanns, E. (1985) Mn^{3+} in garnets, III. Absence of Jahn-Teller distortion in synthetic Mn^{3+} -bearing garnet. *Physics and Chemistry of Minerals*, 12, 279–282.
- Aubry, A., Dusauroy, Y., Laffaille, A., and Protas, J. (1969) Détermination et étude de la structure cristalline de l'henritermierite, hydrogrenat de symétrie quadratique. *Bulletin Société française Minéralogie et Cristallographie*, 92, 126–133.
- Basso, R. (1987) The crystal structure of palenzonaite, a new vanadate garnet from Val Graveglia (Northern Apennines, Italy). *Neues Jahrbuch für Mineralogie Monatshefte*, 3, 134–144.
- Becker, P.J. and Coppens, P. (1974) Extinction within the limit of validity of the Darwin transfer equations. I. General formalisms for primary and secondary extinction and their application to spherical crystals. *Acta Crystallographica A*, 30, 129–147.
- Blessing, R.H. (1987) Data reduction and error analysis for accurate single crystal diffraction intensities. *Crystallography Reviews*, 1, 3–58.
- Breuer, K.H. and Eysel, W. (1983) $\text{Ca}_3\text{Mn}_2\text{Ge}_3\text{O}_{12}$. In *The Powder Diffraction File*, card 34–285. International Centre for Diffraction Data.
- Burnham, C.W. (1966) Computation of absorption corrections and the significance of end effects. *American Mineralogist*, 51, 159–167.
- Creagh, D.C. and McAuley, W.J. (1992) X-ray dispersion correction. In Wilson, A.J.C. *International Tables for Crystallography C*, 206–219. Kluwer Academic Publishers, Dordrecht.
- Deer, W.A., Howie, R.A., and Zussman, J. (1982) *Rock-forming minerals Vol. 1A Orthosilicates*. Longman, London.
- Devignes, J.M. and LeGall, H. (1978) Flux growth of single magnetic sublattice antiferromagnetic garnets $\text{Ca}_3\text{Fe}_2\text{Ge}_3\text{O}_{12}$ and $\text{Ca}_3\text{Mn}_2\text{Ge}_3\text{O}_{12}$. *Material Research Bulletin*, 13, 141–146.
- Englman, R. (1972) *The Jahn-Teller effect in molecules and crystals*. John Wiley Interscience, New York.
- Eremenko, V.V., Kharchenko, N.F., Gnatchenko, S.L., Milner, A.A., Sofroneev, S.V., Le Gall, H., Devignes, J.M., and Feldmann, P. (1986) Magneto-optical determination of the MnGeG magnetic point group. *Journal of Magnetism and Magnetic Materials*, 54–57, 1397–1398.
- Finger, L.W. and Prince, E. (1975) A system of Fortran IV computer programs for crystal structure computations. U.S. National Bureau of Standards Technical Note, 854, 128.
- Fujino, K., Momoi, H., Sawamoto, H., and Kumazawa, M. (1986) Crystal structure and chemistry of MnSiO_3 tetragonal garnet. *American Mineralogist*, 71, 781–785.
- Fursenko, B.A. (1983) Synthesis of new high-pressure silicate garnets $\text{Mn}_3\text{M}_2\text{Si}_3\text{O}_{12}$ ($M = \text{V}, \text{Mn}, \text{Ga}$). *Doklady Academy Nauk SSSR*, 268, 421–424.
- Gnatchenko, S.L., Eremenko, S.V., Sofroneev, N.F., Kharchenko, M., Devignes, M., Feldmann, P., and LeGall, A. (1986) Spontaneous phase transitions and optical anisotropy in manganese germanium garnet ($\text{Ca}_3\text{Mn}_2\text{Ge}_3\text{O}_{12}$). *Soviet Physics Journal of Experimental and Theoretical Physics*, 63, 102–109.
- Grant, D.F. and Gabe, E.J. (1978) The analysis of single-crystal Bragg reflections from profile measurements. *Journal of Applied Crystallography*, 11, 114–120.
- Graeff, W., Kub, J., and Wieteska, K. (1991) Ferrielastic Domain Structure Study in $\text{Ca}_3\text{Mn}_2\text{Ge}_3\text{O}_{12}$ Garnet. *physica status solidi (a)*, 126, 477–484.
- Griffen, T.D. and Hatch, D.M. (1992) Crystal chemistry of birefringent silicate garnets: A review. *Trends in Mineralogy*, 1, 269–279.
- Hammonds, K.D., Bosenick, A., Dove, M.T., and Heine, V. (1998) Rigid unit modes in crystal structures with octahedrally coordinated atoms. *American Mineralogist*, 83, 476–479.
- Heinemann, S., Seifert, F., Sharp, T., and Rubie, D. (1997) The cubic-tetragonal phase transition in the system majorite ($\text{Mg}_3\text{Si}_4\text{O}_{12}$)–pyrope ($\text{Mg}_3\text{Al}_2\text{Si}_3\text{O}_{12}$) and garnet symmetry in the Earth's transition zone. *Physics and Chemistry of Minerals*, 24, 206–221.
- Hoffmann, C., Armbruster, T., and Kunz, M. (1997) Structure refinement of (001) disordered gaudefroyite $\text{Ca}_3\text{Mn}^{3+}_3[(\text{BO}_3)_3(\text{CO}_3)_3\text{O}_3]$: Jahn-Teller distortion in edge-sharing chains of Mn^{3+}O_6 octahedra. *European Journal of Mineralogy*, 9, 7–19.

- Hofmeister, A.M., Scaal, R.B., Campbell, K.R., Berry, S.L., and Fagan, T.J. (1998) Prevalence and origin of birefringence in 48 garnets from the pyrope-almandine-grossularite-spessartine quaternary. *American Mineralogist*, 83, 1293–1301.
- Jahn, H.A. and Teller, E. (1937) Stability of polyatomic molecules in degenerate electronic states. *Proceedings of the Royal Society Serandum A*, 161, 220–235.
- Jarosch, D. (1987) Crystal structure refinement and reflectance measurements of hausmannite, Mn_3O_4 . *Mineralogy and Petrology*, 37, 15–23.
- Kazei, Z.A., Mill, B.V., and Sokolov, V.I. (1977) Cooperative Jahn-Teller effect in the garnet $\text{Ca}_3\text{Mn}_2\text{Ge}_3\text{O}_{12}$. *Journal of Experimental and Theoretical Physics Letters*, 24, 203–206.
- Kazei, Z.A., Novak, P., and Sokolov, V.I. (1982) Cooperative Jahn-Teller effect in the garnets. *Soviet Physics Journal of Experimental and Theoretical Physics*, 56, 854–864.
- Kharchenko, N.F. and Bedarev, V.A. (1993) Effect of nonlinear polarization of light on magnetization reversal in an antiferromagnetic Ca-Mn-Ge garnet crystal. *Low Temperature Physics*, 19, 72–78.
- King, H.E. and Finger, L.W. (1979) Diffracted beam crystal centering and its application to high-pressure crystallography. *Journal of Applied Crystallography*, 12, 374–378.
- Maslen, E.N., Fox, A.G., and O’Keeffe, M.A. (1992) X-ray scattering. In Wilson, A.J.C. *International Tables for Crystallography C*, 476–509. Kluwer Academic Publishers, Dordrecht.
- Miletich, R., Allan D.R., and Angel, R.J. (1998) Structural control of polyhedral compression in synthetic braunite, $\text{Mn}^{2+}\text{Mn}^{3+}\text{O}_8\text{SiO}_4$. *Physics and Chemistry of Minerals*, 25, 183–192.
- Nakatsuka, A., Yoshiasa, A., Yamanaka, T., and Ito, E. (1999) Structure refinement of a birefringent Cr-bearing $\text{Mg}_3(\text{Mg}_{0.34}\text{Si}_{0.34}\text{Al}_{0.18}\text{Cr}_{0.14})_2\text{Si}_3\text{O}_{12}$. *American Mineralogist*, 84, 199–202.
- Nishizawa, H. and Koizumi, M. (1975) Synthesis and Infrared Spectra of $\text{Ca}_3\text{Mn}_2\text{Si}_3\text{O}_{12}$ and $\text{Ca}_3\text{B}_2\text{Si}_3\text{O}_{12}$ (B: Al, Ga, Cr, V, Fe, Mn) Garnets. *American Mineralogist*, 60, 84–87.
- Novak, G.A. and Gibbs, G.V. (1971) The crystal chemistry of the silicate garnets. *American Mineralogist*, 56, 791–825.
- Pabst, A. (1936) The crystal structure of plazolite. *American Mineralogist*, 21, 861–868.
- Palmer, D.C., Putnis, A., and Salje, E.K.H. (1988) Twinning in Tetragonal Leucite. *Physics and Chemistry of Minerals*, 16, 298–303.
- Plumier, R. (1971) Détermination par Diffraction des Neutrons de la Structure antiferromagnétique du grenat $\text{Ca}_3\text{Mn}_2\text{Ge}_3\text{O}_{12}$. *Solid State Communications*, 9, 1723–1725.
- Plumier, R. and Estève, D. (1979) Reinvestigation of the magnetic structure of $\text{Ca}_3\text{Mn}_2\text{Ge}_3\text{O}_{12}$. *Solid State Communications*, 31, 921–925.
- Prandl, W. (1972) Magnetic structure and space group of the garnet $\text{Ca}_3\text{Fe}_2(\text{GeO}_4)_3$. *Solid State Communications*, 10, 529–531.
- Prewitt, C.T. and Sleight, A.W. (1969) Garnet-Like Structures of High-Pressure Cadmium Germanate and Calcium Germanate. *Science*, 163, 386–387.
- Ralph, R.L. and Finger, L.W. (1982) A computer program for refinement of crystal orientation matrix and lattice constants from diffractometer data with lattice symmetry constraints. *Journal of Applied Crystallography*, 15, 537–539.
- Rickwood, P.C. (1968) On recasting analyses of garnet into end-member molecules. *Contributions to Mineralogy and Petrology*, 18, 175–198.
- Ross, N.L., Akaogi, M., Navrotsky, A., Susaki, J., and McMillan, P. (1986) Phase transitions among the CaGeO_3 polymorphs (wollastonite, garnet and perovskite structures): studies by high-pressure synthesis, high-temperature calorimetry and vibrational spectroscopy and calculation. *Journal of Geophysical Research*, 91, 4685–4696.
- Salje, E.K.H. (1990) Phase transitions in ferroelastic and co-elastic crystals. Cambridge University Press, Cambridge.
- Sapriel, J. (1975) Domain-wall orientations in ferroelastics. *Physical Review B*, 12, 5128–5140.
- Shannon, R.D. (1976) Revised effective ionic radii and systematic studies of interatomic distances in halides and chalcogenides. *Acta Crystallographica A*, 32, 751–767.
- Shannon, R.D., Gumeran, P.S., and Chenavas, J. (1975) Effect of octahedral distortion on mean Mn^{3+} -O distances. *American Mineralogist*, 60, 714–716.
- Strens, R.G.J. (1965) Instability of garnet $\text{Ca}_3\text{Mn}_2\text{Si}_3\text{O}_{12}$ and substitution $\text{Mn}^{3+}=\text{Al}$. *Mineralogical Magazine*, 35, 547–549.
- Sugg, B., Gnatchenko, S.L., Faust, B., and Rupp, R.A. (1995) Optical properties of $\text{Ca}_3\text{Mn}_2\text{Ge}_3\text{O}_{12}$. *Applied Physics Letters*, 67, 766–767.
- Sugg, B., Gnatchenko, S.L., and Rupp, R.A. (1996) Holographic reading at 633 nm in the garnet $\text{Ca}_3\text{Mn}_2\text{Ge}_3\text{O}_{12}$. *Journal of the Optical Society of America B*, 13, 2662–2670.
- Toledano, J.-C. and Toledano, P. (1987) *The Landau Theory of Phase Transitions*. World Scientific, Singapore.

MANUSCRIPT RECEIVED MAY 17, 1999

MANUSCRIPT ACCEPTED FEBRUARY 10, 2000

PAPER HANDLED BY LEE A. GROAT